Autonomous translocation and intracellular trafficking of the cell-penetrating and immune-suppressive effector protein YopM

ARTICLE *in* CELLULAR AND MOLECULAR LIFE SCIENCES CMLS · JULY 2013

Impact Factor: 5.81 · DOI: 10.1007/s00018-013-1413-2 · Source: PubMed

6 AUTHORS, INCLUDING:

Lilo Greune
University of Münster
24 PUBLICATIONS **683** CITATIONS

SEE PROFILE

Christian Rüter
University of Münster
15 PUBLICATIONS **92** CITATIONS

SEE PROFILE

Cell. Mol. Life Sci.
DOI 10.1007/s00018-013-1413-2

Cellular and Molecular Life Sciences

RESEARCH ARTICLE

Autonomous translocation and intracellular trafficking of the cell-penetrating and immune-suppressive effector protein YopM

Julia Scharnert · Lilo Greune · Dagmar Zeuschner · Marie-Luise Lubos · M. Alexander Schmidt · Christian Rüter

Received: 27 February 2013 / Revised: 10 June 2013 / Accepted: 21 June 2013

Abstract Extracellular Gram-negative pathogenic bacteria target essential cytoplasmic processes of eukaryotic cells by using effector protein delivery systems such as the type III secretion system (T3SS). These secretion systems directly inject effector proteins into the host cell cytoplasm. Among the T3SS-dependent Yop proteins of pathogenic *Yersinia*, the function of the effector protein YopM remains enigmatic. In a recent study, we demonstrated that recombinant YopM from *Yersinia enterocolitica* enters host cells autonomously without the presence of bacteria and thus identified YopM as a novel bacterial cell-penetrating protein. Following entry YopM down-regulates expression of pro-inflammatory cytokines such as tumor necrosis factor α. These properties earmark YopM for further development as a novel anti-inflammatory therapeutic. To elucidate the uptake and intracellular targeting mechanisms of this bacterial cell-penetrating protein, we analyzed possible routes of internalization employing ultra-cryo electron microscopy. Our results reveal that under physiological conditions, YopM enters cells predominantly by exploiting endocytic pathways. Interestingly, YopM was detected free in the cytosol and inside the nucleus. We could not observe any colocalization of YopM with secretory membranes, which excludes retrograde transport as the mechanism for cytosolic release. However, our findings indicate that direct membrane penetration and/or an endosomal escape of YopM contribute to the cytosolic and nuclear localization of the protein. Surprisingly, even when endocytosis is blocked, YopM was found to be associated with endosomes. This suggests an intracellular endosome-associated transport of YopM.

Keywords *Yersinia* outer protein M · Effector protein · Cell-penetrating protein · Electron microscopy · Intracellular trafficking

Abbreviations

CCV	Clathrin-coated vesicles
CF	Cytosolic fraction
CPP	Cell-penetrating protein
CYT	Cytosol
E	Endosomes
EE	Early endosome
ER	Endoplasmic reticulum
GA	Golgi apparatus
HM	Heavy membranes
LE	Late endosome
LYS	Lysosome
MITO	Mitochondria
MVB	Multi-vesicular-bodies
nCCV	Non-clathrin-coated vesicles
N	Nucleus
NE	Nuclear envelope
NF	Nuclear fraction
PM	Plasma membrane
PNS	Post-nuclear supernatant

M. A. Schmidt and C. Rüter contributed equally to this work.

Electronic supplementary material The online version of this article (doi:10.1007/s00018-013-1413-2) contains supplementary material, which is available to authorized users.

J. Scharnert · L. Greune · M.-L. Lubos · M. Alexander Schmidt · C. Rüter (✉)
Center for Molecular Biology of Inflammation (ZMBE), Institute of Infectiology, Von-Esmarch-Str. 56, 48149 Münster, Germany
e-mail: rueterc@uni-muenster.de

D. Zeuschner
Electron Microscopy Facility, Max-Planck-Institute for Molecular Biomedicine, Röntgenstr. 20, 48149 Münster, Germany

Published online: 09 July 2013

PTD	Protein transduction domain
SE	Sorting endosome
TC	Transport carrier
TGN	Trans-Golgi network
YopM	*Yersinia* outer protein M

Introduction

The type III secretion systems (T3SS) of pathogenic Gram-negative bacteria act as "molecular syringes" by injecting effector proteins directly into the cytoplasm of host cells to modify cellular functions and thus contribute to the extracellular survival of the bacteria. Pathogenic *Yersinia* species (*Y. enterocolitica*, *Y. pestis*, and *Y. pseudotuberculosis*) translocate six different *Yersinia* outer proteins (Yops) via the T3SS into the host cell cytoplasm (YopM, YopE, YopT, YopO/YpkA, YopH, and YopP/YopJ) [1, 2]. These effector proteins are mostly injected contact-dependent into cells, however, in permissive environmental conditions, such as the deprivation of Ca^{2+}, non-contact-dependent secretion of T3SS-effector proteins into the environment can be induced.

YopM is the only known Yop without enzymatic activity and its mode of molecular action is still unclear. The protein consists of two N-terminal α-helices followed by a variable number of 13–21 leucine-rich repeat (LRR) motifs depending on the *Yersinia* species and strain [3]. Analysis of the three-dimensional structure of the *Y. pestis* YopM revealed a horseshoe-like shape. Following the T3SS-mediated translocation into the host cell, a directed transport to the nucleus via a vesicle-associated pathway has been described [4]. The YopM sequence of *Y. enterocolitica* harbors two putative nuclear localization signals (NLS) in LRR 1-3 and in the C-terminal 32 amino acid residues [5]. The mechanism of YopM translocation into the nucleus has not yet been elucidated although a carrier-mediated transport has been suggested [4]. In a murine *Y. pestis* infection model, YopM is associated with a global depletion of natural killer (NK) cells [6] and a reduced recruitment of antibacterial host cells [7]. Macrophages and NK cells isolated from the spleen and liver tissues of infected mice show a reduced expression of several pro-inflammatory cytokines (e.g., TNF-α) [6]. This in vivo observation raises the challenging question of how a locally injected effector protein can exert global effects on host cell immune responses.

In this context, we recently identified the *Y. enterocolitica* T3SS-secreted effector protein YopM as a novel cell-penetrating protein (CPP), which can translocate into target cells autonomously without any need for bacteria or any bacterial factors by penetrating the plasma membrane (PM) [8]. Cell membranes represent complex borders acting likewise as a gateway and a barrier thereby establishing the integrity of a cell and its organelles. Therefore, cell-penetrating peptides or proteins are currently under intense investigation as they are able to translocate also cargo across membrane barriers [9]. However, so far the cell-entry mechanisms of CPPs remain largely elusive. It has been suggested that CPPs are able to directly translocate across cellular membranes in an energy- and receptor-independent way [10]. In addition, several studies have indicated that different endocytic mechanisms, including clathrin-mediated endocytosis [11], caveolae-mediated endocytosis [12], or macropinocytosis [13, 14] can be involved in the uptake of CPPs. Presumably, most CPPs are able to use different routes of translocation simultaneously [15]. Furthermore, it has been shown that the endocytic entry route of a particular CPP depends not only on its structure, physicochemical properties [16], and its concentration on the cell surface, but also on the properties of the attached cargo molecule [17]. Thus far, CPPs and/or their protein transduction domains (PTD) have been mainly derived from eukaryotic or viral proteins, which later served as templates for the design of synthetic CPPs [12].

In our previous work [8], we have identified and characterized YopM derived from *Y. enterocolitica* as the first CPP derived from Gram-negative bacteria. Furthermore, we demonstrated the ability of recombinant YopM to autonomously enter different eukaryotic target cell types including immune and epithelial cells. Our data supported a model in which extracellularly added recombinant YopM undergoes endocytosis involving early or sorting endosomes, which then sort to late endosomes. At later time points, YopM is enriched in the perinuclear region and can also be found inside the nucleus [6]. Strikingly, we found that autonomously translocated YopM remains functional and down-regulates the expression of several pro-inflammatory cytokines including tumor necrosis factor α (TNF-α), a key cytokine in many inflammatory diseases [8]. However, the mechanisms employed by YopM to overcome cellular barriers, reach the cytoplasm and the nucleus have remained elusive.

Here, we investigated the uptake and intracellular trafficking of cell-penetrating recombinant YopM from *Y. enterocolitica* strain 8081 (serotype 0:8; biotype 1B) using HeLa cells as model cells. For this, we employed high-resolution transmission electron microscopy (TEM), which proved to be essential for the characterization of cellular compartments involved in YopM trafficking. We found that under physiological conditions, YopM enters target cells predominantly by exploiting endocytic pathways. The cellular localization of YopM was mapped employing confocal laser-scanning fluorescence microscopy (CLSM) and cell fractionation experiments combined with specific compartmental markers. After 1 h of incubation, YopM was found to be completely absent at secretory membranes, which made the secretory pathway a target for the cytosolic release of

the protein unlikely. However, YopM was detected free in the cytoplasm and likewise in the nucleoplasm. To reach these compartments, YopM either has to escape from the endosomes or directly penetrate the PM. Our results indicate that YopM has the ability to directly traverse the PM in an endocytosis-independent manner.

Materials and methods

Cell culture

HeLa cells were obtained from the German Resource Centre of Biological Material (DSMZ, Braunschweig, Germany) and maintained in DMEM supplemented with 10 % fetal bovine serum, 5 % non-essential amino acids, 1 mM glutamine and antibiotics (PAA) at 37 °C in a 5 % CO_2 atmosphere. The medium was replaced every 2–3 days.

Plasmid construction and protein purification

The generation of $YopM_{N\text{-}367}$ from pYVe8081 virulence plasmid of *Y. enterocolitica* strain 8081 (serotype 0:8; biotype 1B) and its deletion construct $YopM_{87\text{-}C}$ has been described previously [18]. The Tat-GFP fusion protein with a C-terminal 6 × His tag was constructed by inserting the nucleotide sequence encoding the PTD of Tat using oligonucleotides (5′-3′ TATGATGTGCGGCCG TAAGAAACGTCGCCAGCGTCGCCGTCCGCCGC AATGCG and 3′-5′ CTAGCGCATTGCGGCGGACGGCG ACGCTGGCGACGTTTCTTACGGCCGCACA GCA) via NdeI and NheI restriction sites into pET-GFP [8]. For expression and to facilitate affinity purification, YopM and Tat-GFP were transcriptionally fused with a C-terminal 6 × His tag using the plasmid pET24b(+). Expression and purification of recombinant proteins was performed as described [18]. Affinity-purified proteins were dialyzed against PBS and concentrated using Centricon centrifugal filters (Merck Millipore).

Transmission electron microscopy

Gold conjugation of recombinant YopM from *Y. enterocolitica* (pYV8081) was performed as described previously [19]. Cells were incubated with recombinant gold-labeled or free YopM (25 µg/ml) for 1 h at 37 °C. Subsequently, HeLa cells were fixed with 2 % paraformaldehyde (PFA), 0.2 % glutaraldehyde in 0.1 M phosphate buffer, pH 7.4. For cryo-immuno EM, cells were initially fixed in 2 % PFA and 0.2 % glutaraldehyde in 0.1 M phosphate buffer, pH 7.4 according to Mari et al. [20]. In brief, for internalization, HeLa cells grown on culture dishes were incubated with YopM for 1 h. At this time, the medium was replaced and double-fixative was directly added for 10 min and then exchanged against 1 × fixative for an additional 3 h. The monolayer was washed with 0.1 M phosphate buffer (pH 7.4), scraped carefully in 2 % gelatine, in 0.1 M phosphate buffer, subsequently centrifuged, and resuspended into 12 % gelatine. The embedded cells were solidified on ice and dissected into small cubes. The material was immersed in 2.3 M sucrose for infiltration and cryo-protection, mounted, and finally frozen in liquid N_2 for long-time storage. Trimming and ultrathin cryo-sectioning of 50 nm sections was performed at −110 °C in a cryo-chamber of an ultra-microtome (UC6, Leica, Vienna, Austria). The sections were subjected to immunoelectron microscopy labeling with the indicated antibodies, SNX1 (BD Biosciences) and α-YopM (polyclonal rabbit antibody). Bound antibodies were detected using protein-A-gold of different sizes (Cell Microscopy Center—CMC, Utrecht, The Netherlands) according to the published protocol [20]. The samples were analyzed at 80 kV using a transmission electron microscope (Tecnai 12-biotwin, FEI Deutschland, Germany). Selected areas were documented with digital imaging plates (Ditabis). For quantification, we randomly selected 50 cell profiles on sections of two different biological samples. The antibody signals were enumerated as the amount of gold particles linked to certain cellular compartments. Total numbers were corrected by subtracting the number of gold particles counted in 50 cell profiles of the negative control (non-incubated HeLa cells, treated the same way as the HeLa cells incubated with YopM). The normalized values were expressed in percent and combined in a graph for illustration.

Confocal laser-scanning microscopy

HeLa cells were seeded on glass coverslips in 24-well plates and grown to about 70 % confluency. YopM was labeled using the Cy3 AB labeling kit (GE Healthcare, Waukesha, WI, USA). Prior to incubation with recombinant YopM protein, cells were washed once with PBS and fresh medium containing YopM-Cy3 (25 µg/ml for 1 h at 37 °C and 5 % CO_2, if not indicated otherwise) was added. Subsequently, cells were kept on ice, washed two times with PBS, and once with acid buffer (0.2 M glycine, pH 2) to remove any residual surface-bound proteins [21]. Cells were fixed in 4 % PFA and quenched with 0.2 M glycine for 20 min at room temperature. For permeabilization, cells were incubated with 1 mg/ml saponin in blocking solution (0.1 % BSA, 5 % goat serum in PBS) for 15 min. Cells were incubated with primary and secondary antibodies in 1 mg/ml saponin in 1:10 diluted blocking solution. Cellular structures were visualized using primary antibodies against Rab5, 7, 9 (Cell Signaling Technology, Beverly, MA, USA), Rab11 (Invitrogen, Carlsbad, CA, USA), Rab6 (Santa Cruz

Biotechnology, Santa Cruz, CA, USA) and SNX1 (BD Biosciences, Franklin Lakes, NJ, USA) according to the manufacturer's instructions. The mouse monoclonal antibodies against human lysosome-associated membrane protein 3 (LAMP3/CD63, clones H5C6) were obtained from the Developmental Studies Hybridoma Bank (University of Iowa, Iowa City, IA, USA). Cy2-labeled secondary antibodies were purchased from Dianova. DNA was stained with DRAQ5 (Biostatus). Glass coverslips were mounted in Fluorescence Mounting Medium (Dako, Carpinteria, CA, USA). All preparations were analyzed using confocal laser-scanning microscopy (LSM 510 META microscope, equipped with a Plan-Apochromat 63 x/1.4 oil immersion objective; Carl Zeiss, Oberkochen, Germany).

Cytoplasmic and nuclear protein extraction

HeLa cells were seeded in 100-mm cell culture dishes. Cells were washed with PBS and after addition of fresh medium were incubated for 1 h with recombinant YopM (25 μg/ml). Following incubation, the cells were washed twice with PBS. Cytoplasmic and nuclear protein extracts were prepared using NE-PER Nuclear and Cytoplasmic Extraction Reagents (Thermo Fisher Scientific, Waltham, MA, USA) following the manufacturer's instructions and analyzed by immunoblot analysis. In order to assess the purity of the fractions, both were analyzed using antibodies against α-tubulin (Sigma-Aldrich, St. Louis, MO, USA) and lysine-specific demethylase 1 (LSD-1) (Cell Signaling Technology). The presence of YopM in cytosolic and nuclear fractions was assessed using a YopM-specific polyclonal rabbit antibody. Immunoblots were analyzed using Lumi-Imager T1 and Lumi Analyst software (Roche Diagnostics, Basel, Switzerland). For statistical analysis, a Student's *t* test was performed and *p* values were calculated applying the unpaired two-tailed test using Excel (Microsoft, Redmond, WA, USA).

Fractionation of endosomal membranes

Sub-cellular fractionation was carried out using a discontinuous sucrose flotation gradient as described [22]. Briefly, cells were homogenized in homogenization buffer (3 mM imidazole–HCl, pH 7.4, 0.25 M sucrose) and a post-nuclear supernatant (PNS) was prepared. The PNS was adjusted to 40.6 % sucrose and loaded at the bottom of an SW60 centrifuge tube. To prepare a one-step gradient, the PNS was overlaid with a 35 % sucrose solution in 3 mM imidazole–HCl, pH 7.4, and finally filled up with homogenization buffer. The gradient was centrifuged for 1.5 h at 35,000 × *g* at 4 °C. Endosomes and heavy membranes were collected at the respective gradient interfaces. Protein concentrations were measured using the BCA Protein Assay method (Thermo Fisher Scientific) and samples were analyzed by immunoblotting using primary antibodies against Rab5, Rab7, PDI (Cell Signaling Technology), TfR (Invitrogen), and anti-GFP polyclonal serum (Invitrogen). Additionally, for negative staining of endosomes for EM, 5 μl of each fraction were placed on a copper grid and incubated at room temperature for 10 min. After removal of excess liquid, phosphotungstic acid (pH 7) was added for negative staining. The purity and integrity of the endosomal membrane preparations were assessed by TEM as described above.

FACS analysis

HeLa cells were seeded in 100-mm cell culture dishes and cultured until 90 % confluence. Cells were washed with PBS and incubated for 15 min with 500 μg/ml proteinase K (Sigma) to remove cell surface proteins. To monitor transferrin uptake, cells were detached using citrate saline solution (135 mM potassium chloride, 15 mM sodium citrate). Subsequently, cells were washed three times with PBS containing protease inhibitor (Complete Protease Inhibitor Cocktail, Roche Applied Science). Cells were incubated with YopM-Cy3 (25 μg/ml) or transferrin-Alexa 488 (25 μg/ml) for a total of 1 h at 37 °C. To analyze membrane integrity of HeLa cells at 4 °C, cells were incubated with propidium iodide (1 μg/ml) on ice for a total of 1 h with or without YopM-Alexa 488 (25 μg/ml). Samples were taken at different time points and, when indicated, Trypan blue (final concentration 0.2 %) was added directly before measurement to quench extracellular fluorescence. Finally, the cells were analyzed by flow cytometry using a FACScan flow cytometer (BD Biosciences). Fluorescence was assessed from 1×10^4 cells judged to be intact by their forward and side scatter.

Results

Cellular distribution of recombinant YopM in HeLa cells

To follow the internalization route of recombinant cell-penetrating YopM on the ultra-structural level, we needed to identify and illustrate accessible cellular compartments. We chose to use the 1-h time point of constant YopM incubation as this would allow us to depict the cellular distribution of the protein at different stages of penetration at the same time. As a first approach, we incubated HeLa cells for 1 h at 37 °C with YopM conjugated to 6 nm colloidal gold. The gold-labeled protein was found to localize to a high extent in endocytic compartments as well as in the cytoplasm and the nucleus (Fig. 1). In particular, we found that YopM-gold (6 nm) is taken up via clathrin-mediated endocytosis

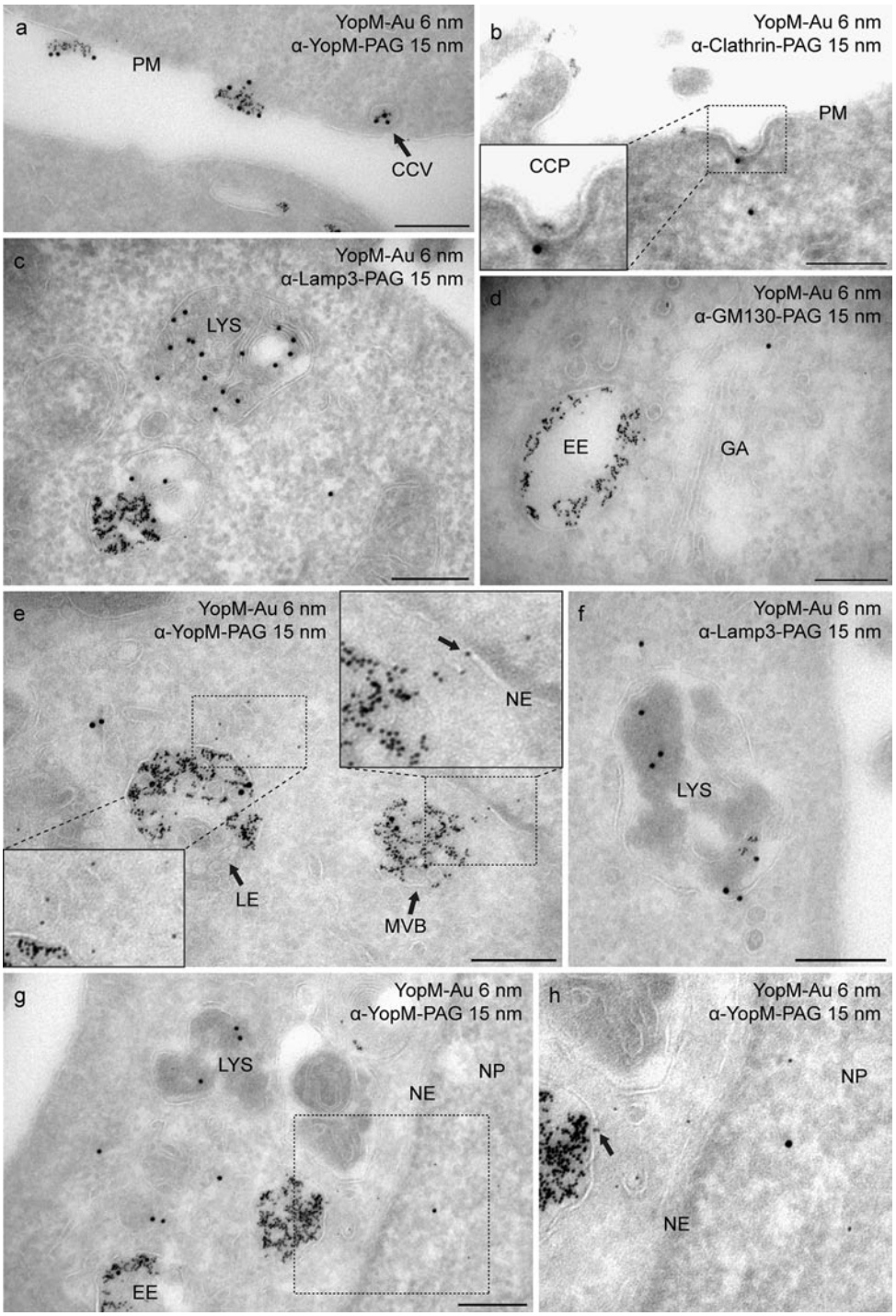

Fig. 1 Cellular distribution of gold-conjugated YopM. HeLa cells were incubated for 1 h with gold-conjugated recombinant YopM and prepared for TEM. To visualize different cellular compartments, ultrathin cryosections were incubated with the indicated antibodies and detected by protein-A-gold (15 nm). The specificity of the YopM-antibody in the EM analysis was evaluated by additional incubation of the sections with the purified polyclonal YopM-antibody detected by PAG (15 nm). **a** YopM-gold (6 nm) is taken up via endocytosis. **b** Clathrin-coated pit containing YopM. **c**, **f** YopM localized to Lamp3-positive (15-nm gold) lysosomal structures. **d** YopM was found accumulated in EE but was never detected on GM130-positive (15-nm gold) structures of the Golgi apparatus. e, g YopM was found free in the cytosol, in close proximity to YopM-loaded endosomal structures (LE, MVB). Parts of the cytosolic YopM seem to traverse the NE and enter the nucleus (see *arrow* in top-right magnification in **e**). **h** Magnification of the *dashed square* in **g**. YopM appears to escape or to be associated with the endosomal membrane (*see arrow*) before it enters the nucleus. *Scale bars*, 200 nm. *CCV* clathrin-coated vesicle, *CCP* clathrin-coated pit, *EE* early endosome, *GA* Golgi apparatus, *LE* late endosome, *LYS* lysosome *MVB* multi-vesicular body, *NE* nuclear envelope, *NP* nucleoplasm, *PAG* protein-A-gold, *PM* plasma membrane

(Fig. 1a, b). After endocytosis, YopM-gold appears to be transported via early endosomes (EE) to late endosomes (LE), where it accumulated (Fig. 1d, e). Interestingly, YopM localized to Lamp3-positive (15-nm gold) lysosomal structures only in minor amounts (Fig. 1c, f) and was never detected on GM130-positive (15-nm gold) structures of the Golgi apparatus (Fig. 1d). Furthermore, YopM-gold was detected free in the cytosol, in close proximity to YopM-containing endosomal structures such as LE and multivesicular bodies (MVB; Fig. 1e). From these endosomes, YopM-gold appears to escape before it traverses the nuclear envelope (NE) and enters the nucleus (Fig. 1g, h). These results indicate that YopM initially enters host cells via a vesicular pathway before entering the cytoplasm at later time points.

However, as it cannot be ruled out that the prior conjugation of gold to YopM might interfere with its biological functions [23] and in particular its mechanism of translocation, we performed immunogold labeling of YopM on ultrathin cryosections as a complementary approach. Even if the detection of translocated YopM by specific antibodies might not be as efficient as direct gold labeling, it ensured a more reliable illustration of the translocation and avoided potential artifacts due to the conjugated gold. The specificity of the anti-YopM antibodies was confirmed by two independent criteria. First, the anti-YopM antibodies detected gold-conjugated YopM (Fig. 1a, e, g). Second, HeLa cells that had not been incubated with YopM showed either no or only negligible background labeling.

HeLa cells were incubated with YopM for 1 h at 37 °C and after immunolabeling the cellular distribution of the protein was analyzed by TEM (Fig. 2). We found specific labeling for YopM at the PM, where it was found to locate in pits between microvilli extensions and in clathrin-coated vesicles (CCV) derived from the PM (typically 200 nm in diameter) (Fig. 2a, b). Additionally, YopM was found in close proximity to the PM in non-clathrin-coated vesicles (nCCV; Fig. 2c). Along the endocytic route, where organelles are easily distinguished based on their characteristic morphologies, labeling appeared in early (EE; Fig. 2d), and late endosomes (LE; Fig. 2e). In addition to the vesicular subset of intracellular YopM, the protein appeared free in the cytoplasm, e.g., underneath the PM (Fig. 2a), and also distributed throughout the cytoplasm, as well as in the nuclear compartment (Fig. 2f, g). These findings pointed to a direct membrane penetration by YopM.

To semi-quantitatively assess the distribution of YopM in various cellular compartments by an unbiased approach, the gold label of defined compartments was enumerated in 50 randomly selected cell profiles. The background labeling found in cells which had not been incubated with YopM (50 randomly selected cell profiles) was subtracted, and the remaining signal was subsequently expressed as percentage of total label (Fig. 2h). After 1 h incubation of HeLa cells with recombinant YopM, the protein was found at the PM (9 %), associated with clathrin-coated vesicles (CCV: 0.9 %), non-clathrin-coated vesicles (nCCV: 3.4 %), transport carriers (TC: 4 %), early endosomes (EE: 12 %), and late endosomes (LE: 18 %). Minor labeling was found in mitochondria (2 %) and other compartments (8 %; Fig. 2h). A major fraction of the protein was detected in the cytoplasm (24 %) and in the nucleus (18.7 %), indicating that already after 1 h of incubation YopM had translocated to these compartments (Fig. 2h).

The role of vesicular transport pathways in intracellular trafficking of YopM

Membrane traffic between cellular organelles is strictly regulated by numerous regulatory proteins. Initially, endocytosed cargo is present in Rab5-containing early endosomal compartments that can undergo maturation to Rab7-containing late endosomes targeted for lysosomes (LYS) or to various recycling compartments to return the cargo to the PM [24, 25]. Rab9, which is localized on LE, is involved in the traffic between LE and TGN [26], whereas Rab6 regulates intra-Golgi traffic [27].

Our results show that endocytosed YopM is intracellularly transported and sorted to different compartments. The protein was found on and in internal vesicles of EE/MVB (Fig. 3a) thus destined for the degradative pathway. Interestingly, YopM was also detected in sorting endosomes (SE) and was found to be partially associated with TC arising from these organelles (Fig. 3c, e). To investigate whether different pathways might be involved in these transport processes of YopM, we incubated HeLa cells with Cy3-labeled YopM for 1 h and visualized its co-localization with compartment-specific marker proteins by CLSM. YopM-Cy3 co-localized with Rab5-containing vesicles (Fig. 3b), but was not found in Rab11-positive compartments (Fig. 3d), indicating that the protein is not returned to the PM via recycling endosomes. Interestingly, YopM could also be detected in distinct endosomal TC profiles (Fig. 3e). As co-localization with Rab9 was not detectable (Fig. 3f), we conclude that late endosomal YopM is not transported to the TGN. Further characterization of these TC revealed that YopM and the retromer component SNX1 [20] localize in close proximity in sorting endosomes (Fig. 4a), which leads to partially overlapping immunofluorescence signals (Fig. 4b). However, at the ultra-structural level of resolution we never could find TC, which were double-labeled for YopM and SNX1. This observation corresponds to the persistent absence of YopM from membranes of the Golgi network (Fig. 4c). Furthermore, YopM does not co-localize with Rab6, a Golgi marker involved in intra-Golgi transport (Fig. 4d).

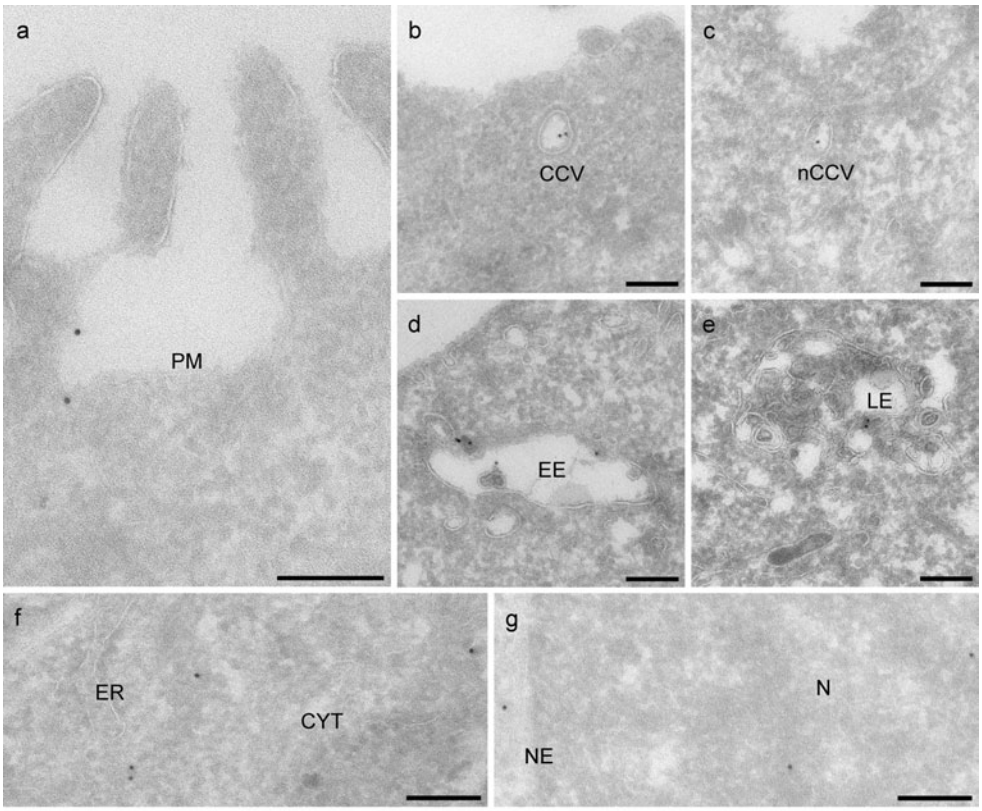

h

Compartment	PM	CCV	nCCV	TC	EE	LE	CYT	N	MITO	others
Rel. distribution of gold particles (%)	9.07	0.85	3.40	3.97	11.90	18.13	24.08	18.70	1.97	7.93

Fig. 2 YopM exploits mostly endocytosis to enter the cell and is located in the cytosol and nucleoplasm. **a**–**g** HeLa cells were incubated for 1 h with recombinant YopM at 37 °C and prepared for cryo-immuno EM. **a** Specific labeling for YopM was detected at the PM, especially in pits between microvilli. **b**, **c** YopM was transported in CCV as well as in nCCV. **d**, **e** YopM was located in EE and LE. **f**, **e** YopM was detected free in the CYT and inside the N. *Scale bars*, 200 nm. **h** Relative sub-cellular distribution of YopM in HeLa cells after 1 h incubation at 37 °C. Fifty cell profiles on sections of two different samples were chosen randomly and the antibody signal was counted as the number of gold particles linked to certain cellular compartments. The total number was corrected by subtracting the number of gold particles counted in 50 random cell profiles of negative controls. The corrected values were expressed in percent. *CCV* clathrin-coated vesicle; *nCCV* non-clathrin-coated vesicle, *CYT* cytosol, *EE* early endosome, *LE* late endosome, *TC* transport carrier, *ER* endoplasmic reticulum, *MITO*, mitochondrion, *N* nucleus, *NE* nuclear envelope, *PM* plasma membrane

Therefore in summary, we conclude that YopM-positive TC do not follow the retrograde transport route via the Golgi apparatus (GA) towards the endoplasmic reticulum (ER).

Along the endocytic route YopM is transported from EE to LE (Fig. 4e, f) and partially also to lysosomal compartments (Fig. 4g), where it co-localizes with the lysosome-associated membrane protein 3 (LAMP3/CD63; Fig. 4h).

Recombinant YopM translocates to the cytosol and into the nucleus

CPPs are able to traverse cellular membranes and several different mechanisms have been proposed to explain their direct translocation across the PM or their escape from endo-lysosomal compartments [28, 29]. A common feature of many of the proposed models is the interaction of CPPs with negatively charged polysaccharides on the cell surface to facilitate their translocation across the lipid bilayer [30]. The results obtained in this study provide evidence that YopM is able to traverse cellular membranes directly. While a fraction of the intracellular protein was detected within vesicular compartments, YopM was also localized free throughout the cytoplasm and inside the nucleus (Fig. 2). Therefore, cytosolic YopM has to overcome the PM or escape from the endosomal network after endocytosis. Here, we have obtained experimental evidence that both routes for the translocation of YopM are possible, as

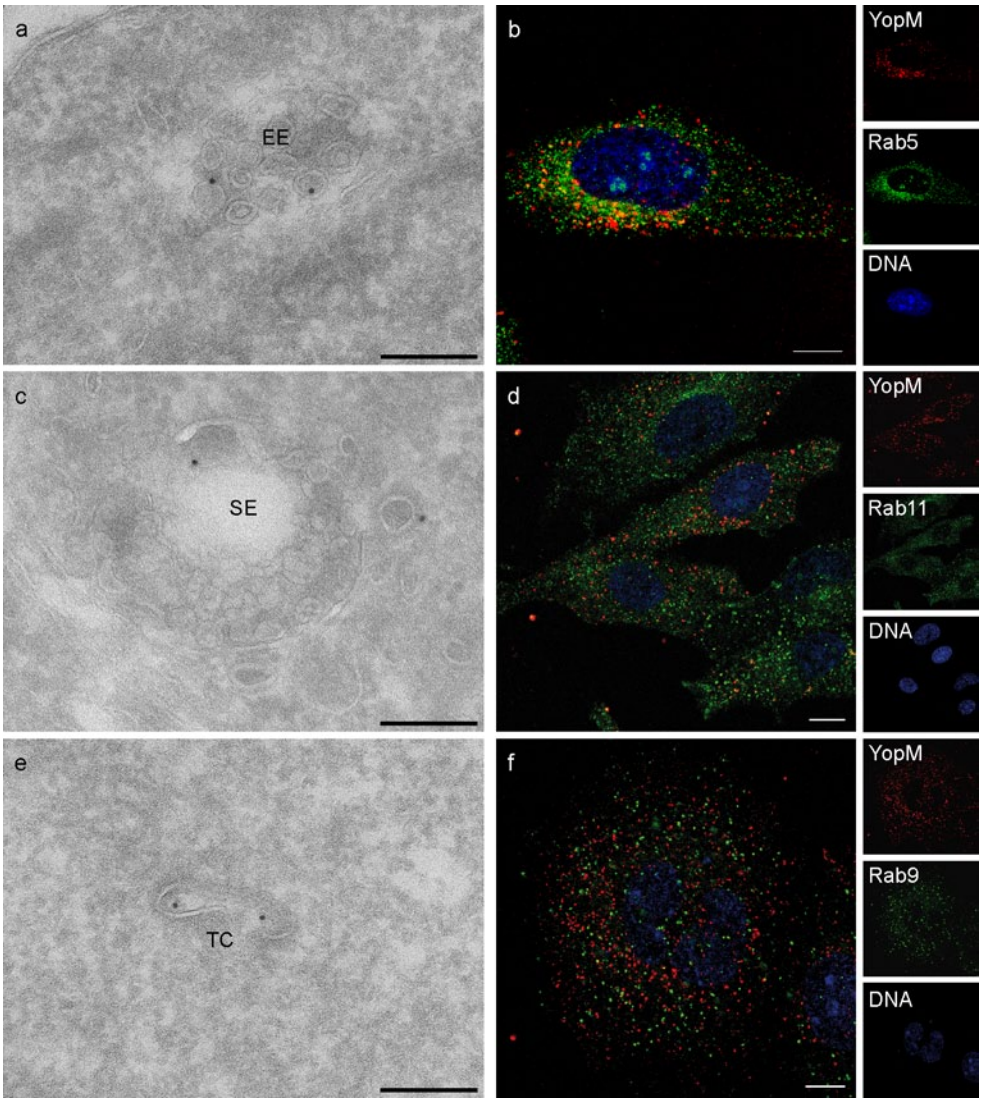

Fig. 3 The role of early endosomes, sorting endosomes, and transport carriers in intracellular trafficking of YopM. **a**, **c**, **e** HeLa cells were incubated for 1 h with recombinant YopM and after immunolabeling visualized by TEM. Besides localization on (**a**) internal vesicles of EE, YopM could be found in (**c**) SE and (**e**) TC. *Scale bars* 200 nm. **b**, **d**, **f** HeLa cells were incubated for 1 h with Cy3-labeled YopM and processed for CLSM. The sub-cellular localization of YopM-Cy3 (*red*) was analyzed in relation to endosomal marker proteins (*green*). DNA was stained with DRAQ5 (*blue*). All three fluorescence images were merged. Single fluorescence channels are represented in the right panel. *Scale bars* 10 μm. **b** YopM co-localized with Rab5-containing early endosomal structures. YopM was not found to localize to recycling endosomes, which where visualized by the marker protein Rab11 or Rab9-containing late endosomal micro-domains. *EE* early endosome, *SE* sorting endosome, *TC* transport carrier

free protein was found underneath the PM, in the cytosol, and at the nuclear envelope (Fig. 5a), as well as near vesicular compartments (Fig. 5b). Interestingly, YopM often appeared to be attached to a membrane (Fig. 5c, d). Whether these observations catch YopM in the act of endosomal escape or represents an interaction of free YopM with the vesicle surface can not yet be resolved. However, an interaction of free YopM with the vesicle surface might enable a directed vesicle-associated transport of cytosolic YopM for example towards the nucleus.

YopM can penetrate cells independent of endocytic mechanisms

The cellular distribution of YopM and specifically its frequent membrane-associated location indicated that in addition to cell-penetration by endocytic pathways the protein might be able to directly traverse cellular membranes. For further analysis, endocytic pathways were inhibited by lowering the incubation temperature to ≤4 °C [30, 31]. In comparison to molecular inhibitors that only block specific

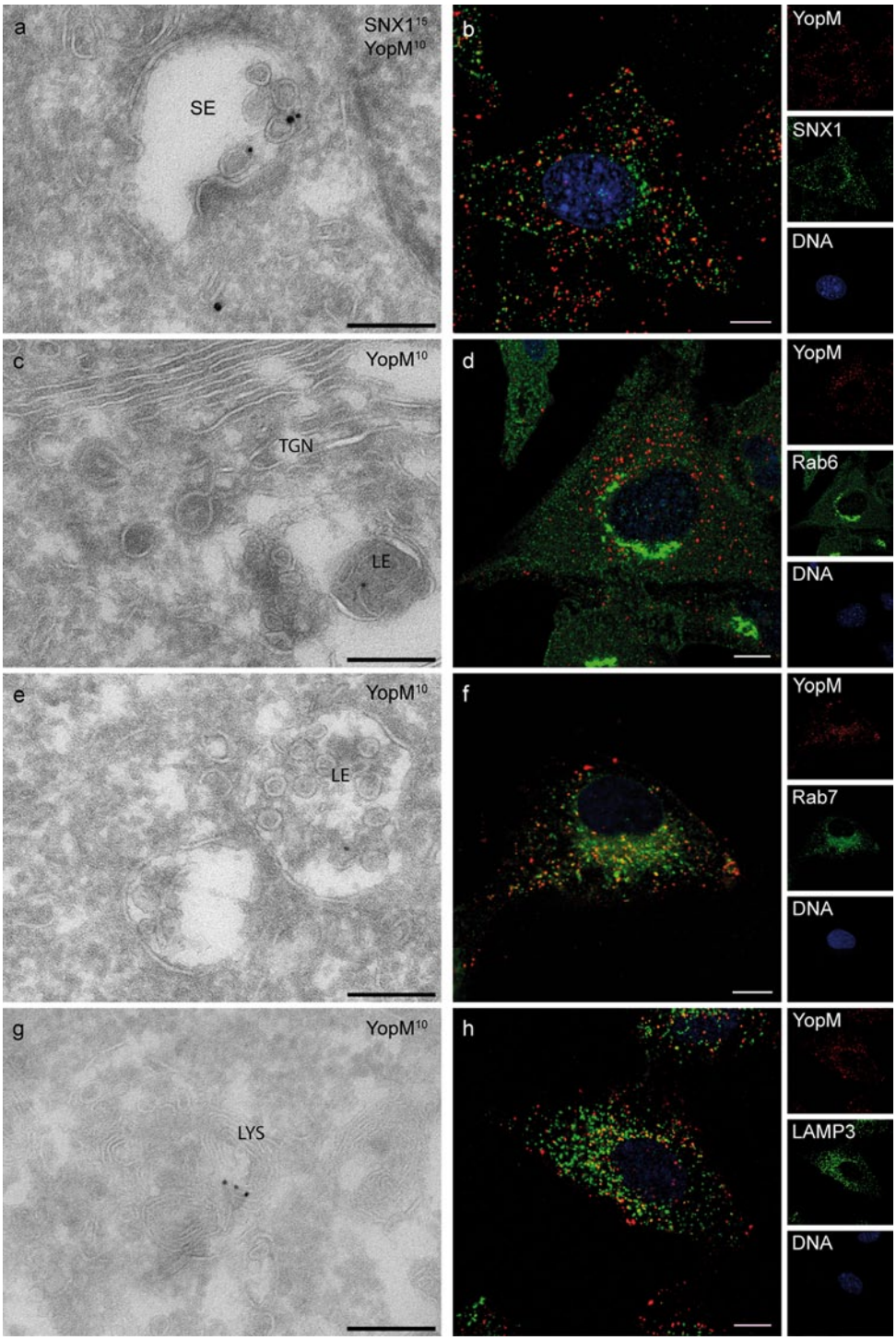

Fig. 4 YopM is not transported to the trans-Golgi network. **a**, **c**, **e**, **g** HeLa cells were incubated for 1 h with recombinant YopM and prepared for TEM. Preparations shown in **a**, **c**, **e**, and **g** were immunogold labeled for YopM, whereas **a** shows a double immunogold labeling for YopM and SNX1. The size of the gold particles is indicated at the top of each micrograph. **a** YopM and SNX1 are in close proximity in sorting endosomes but do not co-localize on identical transport carriers. **c** YopM was never detectable in any part of the Golgi network. **e**, **g** YopM was found in LE as well as in lysosomal compartments. *Scale bars* 200 nm. **b**, **d**, **f**, **h** HeLa cells were incubated for 1 h with Cy3-labeled YopM and prepared for CLSM. The subcellular localization of YopM-Cy3 (*red*) was compared to marker proteins (*green*). DNA was stained with DRAQ5 (*blue*). All three fluorescence images were merged and single fluorescence channels are represented in the right panel. *Scale bars* 10 μm. **b** YopM signals partially overlapped with SNX1 staining. **d** YopM does not co-localize with the Golgi-associated GTPase Rab6. **f**, **h** Co-localization of YopM with the late endosome marker Rab7 and the lysosomal marker Lamp3/CD63 was detectable. *LE* late endosome, *LYS* lysosome, *SE* sorting endosome, *SNX1* sorting nexin 1, *TGN* trans-Golgi network

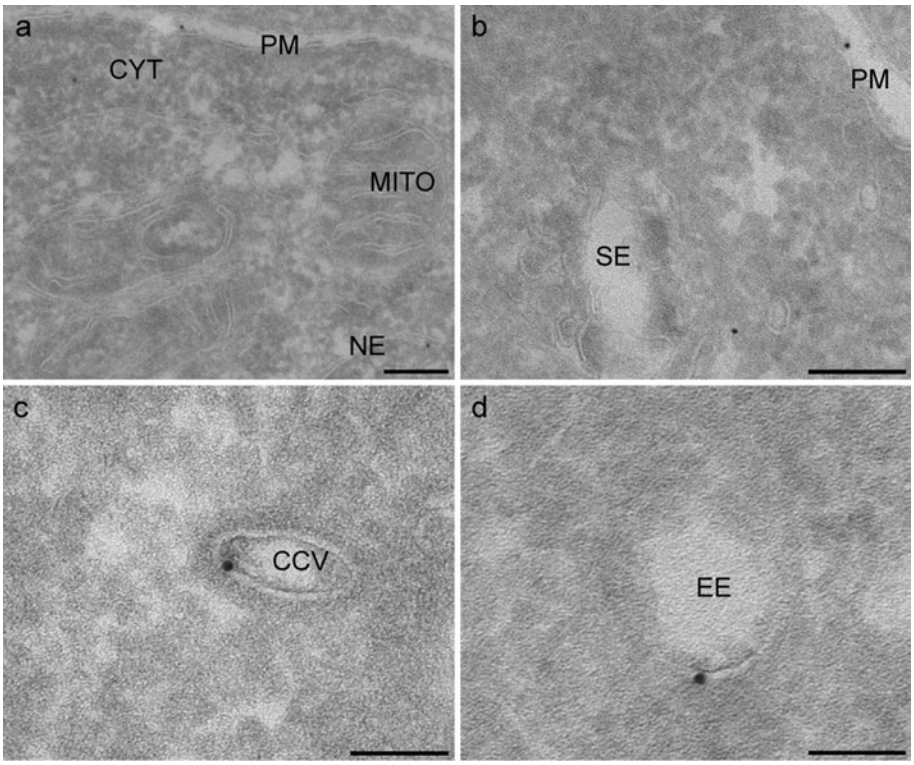

Fig. 5 Extra-endosomal localization of YopM. HeLa cells were incubated for 1 h with recombinant YopM and after immunolabeling visualized by TEM. **a** YopM was found on the outer leaflet of the PM as well as adjacent to the inner PM leaflet free in the cytoplasm and on the nuclear envelope. **b–d** Frequently, the protein was detectable within close distance to vesicular compartments, attached or between the two leaflets of an endosomal membrane. *Scale bars* (**a**, **b**), 200 nm; Scale bars (**c**, **d**), 100 nm. *CCV* clathrin-coated vesicle, *CYT* cytosol, *EE* early endosome, *MITO* mitochondrion, *PM* plasma membrane, *SE* sorting endosome, *NE* nuclear envelope

pathways, temperature-based inhibition has the advantage of blocking all endocytic pathways simultaneously [32, 33]. For this, HeLa cells were incubated with recombinant YopM for 1 h at 4 °C, cryo-sectioned and prepared for immunoelectron microscopy. Enumeration of the immunogold label of YopM in the 4 °C profiles revealed that 29.2 % of the total protein had accumulated at the PM (Fig. 6f), whereas more than three times less PM-associated YopM was detected at 37 °C (Fig. 6g). The amount of intracellular YopM at 4 °C was approximately 75 % lower compared to incubation at the physiological temperature of 37 °C. This observation is consistent with results obtained by previous FACS analysis [8]. However, the increased relative cytosolic localization at 4 °C (32.6 %) in comparison to 37 °C (24 %, Fig. 6h) and the intracellular proximity to the PM clearly show that YopM also translocates to the cell interior in an endocytosis-independent manner. To exclude the possibility that cell penetration of YopM observed at 4 °C was a consequence of a general increase in plasma membrane permeability, we co-incubated the cells with YopM and PI on ice and then quantified PI uptake by flow cytometry. Co-incubation of cells with YopM and PI at 4 °C had no significant effect on the uptake of PI (Fig. S2). This data suggest that incubation of cells with YopM at 4 °C did not induce leakage of the plasma membrane.

In contrast to the uptake of YopM at 37 °C, at 4 °C the protein was not detectable inside the nucleus using TEM. To verify this finding and to rule out false-negative results due to weak immunogold-labeling, we performed subcellular fractionation experiments. After incubation with YopM at 4 and 37 °C, the cells were separated in cytosolic and nuclear fractions and analyzed by Western blotting (Fig. 7a). The results show that at 4 °C YopM is still detectable in the nucleus, albeit in a much lower amount. However, since endocytosis is blocked at 4 °C, this might be attributed to the reduced total amount of intracellular YopM, which in turn causes a diminished amount of protein translocation into the nucleus. Further analysis by densitometry revealed that the cyto-nuclear ratio of YopM was equivalent at 4 and 37 °C (Fig. 7b). Thus, the decreased nuclear YopM can be attributed to a generally reduced amount of cytosolic YopM.

Unexpectedly, even at 4 °C, YopM was found to be associated with CCV (Fig. 6c) and, moreover, also within LE (Fig. 6e). To confirm these observations, endosomes from YopM-incubated cells were isolated and enriched using a discontinuous sucrose gradient. The subcellular distribution of the protein was compared at 4 °C and 37 °C (Fig. 7c). The purity of the different fractions as well as the integrity of the endosomal preparations were assessed by electron microscopic analysis (Fig. 7e) and by the detection of specific marker proteins for the respective cellular compartments. Comparison of the amount of YopM in the post-nuclear supernatant (PNS), which includes all cell organelles and the cytosol without the nuclei, confirmed the strongly decreased ability of YopM to enter cells at

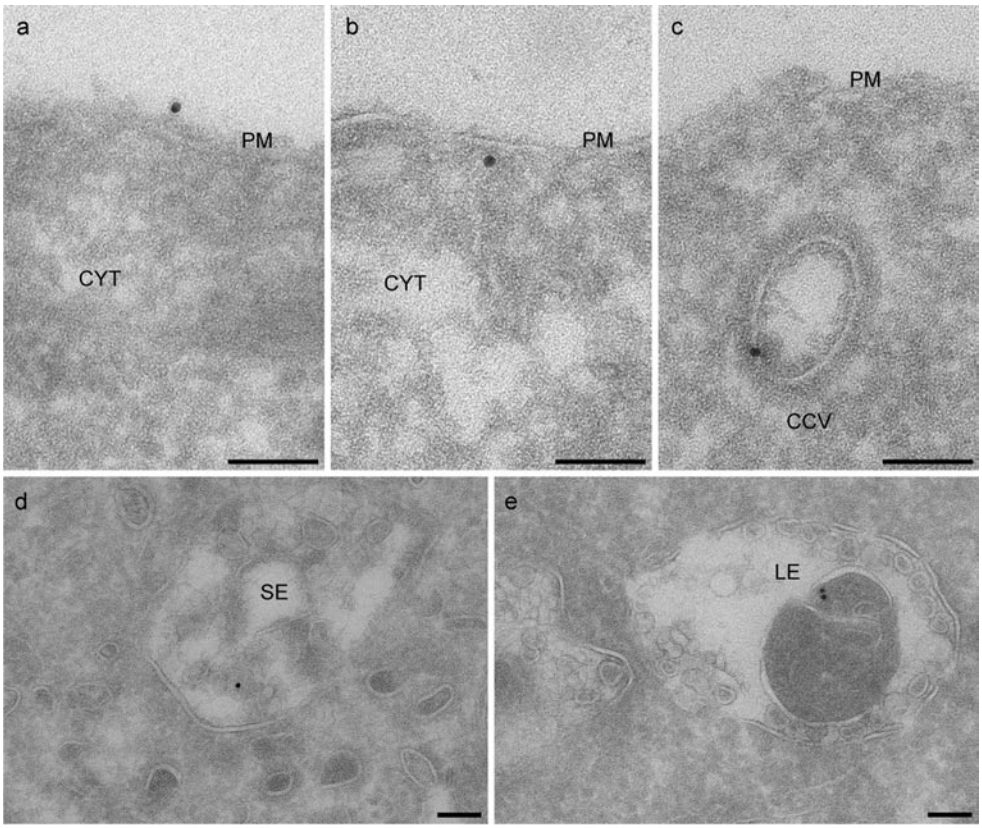

f

Compartment	PM	CCV	nCCV	TC	EE	LE	CYT	N	MITO	others
Rel. distribution of gold particles (%)	29.17	3.47	0.69	2.08	4.17	21.53	32.64	0	0	6.25

g

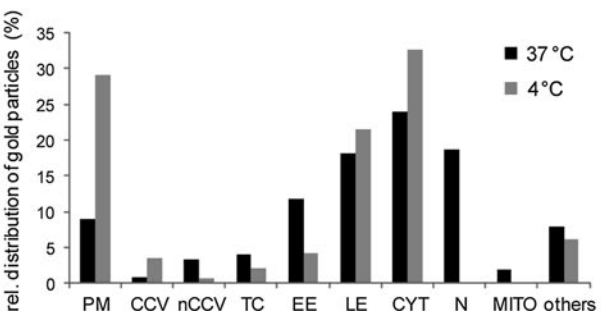

Fig. 6 Incubation of HeLa cells at 4 °C did not abrogate cell penetration by YopM. **a**–**e** HeLa cells were incubated for 1 h with recombinant YopM at 4 °C and after immunolabeling visualized by TEM. **a**, **b** YopM was frequently found attached to the cellular surface and in the cytoplasmic periphery of the PM. **c**-**e** The protein was also detectable associated with CCV, SE, and LE. *Scale bars* 100 nm. **f** Relative subcellular distribution of YopM in HeLa cells after 1 h incubation at 4 °C. Fifty cell profiles on sections of two different samples were randomly selected and the antibody signal was counted as the amount of gold particles linked to certain cellular compartments. The total numbers were corrected by subtracting the number of gold particles counted in 50 cell profiles of the negative control. The corrected values were expressed in percent. **g** Comparison of the relative subcellular distribution of YopM in HeLa cells after 1 h incubation at 37 °C and 4 °C. *CCV* clathrin-coated vesicle, *nCCV* non-clathrin-coated vesicle, *CYT* cytosol, *EE* early endosome, *LE* late endosome, *TC* transport carrier, *MITO* mitochondrion, *PM* plasma membrane, *N* nucleus

4 °C. The heavy membrane (HM) fraction that contains the PM showed an increased YopM signal compared to HM obtained at 37 °C, which is consistent with the EM analysis (Fig. 7c). This indicates that large amounts of the protein remain bound to the PM when endocytosis is blocked. The amount of YopM found in the endosomal fraction clearly illustrates the predominantly endocytic uptake of the protein at physiological temperatures. However, in concert with the findings by TEM, YopM can also be detected in the endosomal fraction at 4 °C. To analyze whether this is YopM-specific or might be observed also with other CPPs such as the transactivator of transcription (Tat) protein of the human immunodeficiency virus type 1 (HIV-1) [34, 35], we repeated the experiments using a Tat-GFP fusion protein. Interestingly, although at 37 °C Tat-GFP was endocytosed in high amounts, resulting in a prominent GFP-signal, we could not detect any Tat-GFP in the endosomal fraction at 4 °C (Fig. 7d). Therefore, we conclude that YopM uses endosomes as transporters to move within the cell, presumably also to reach the nucleus. Even at low temperatures (4 °C) YopM attaches to vesicular and endosomal membranes, demonstrating that this mechanism

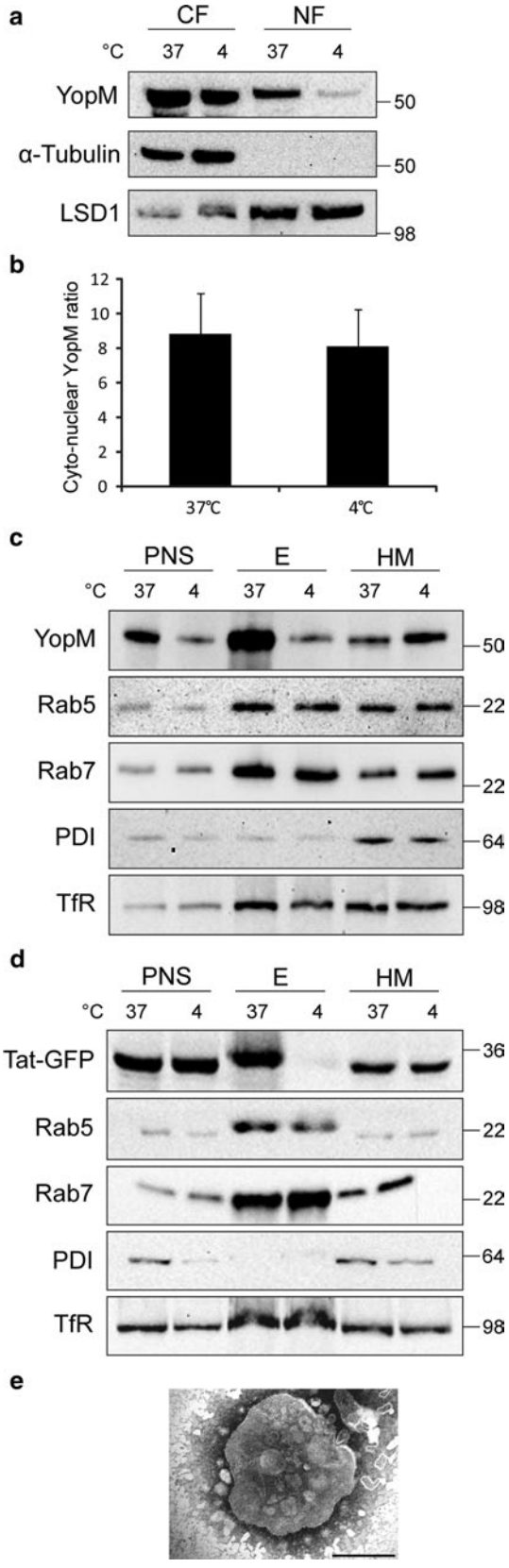

Fig. 7 Uptake of YopM is impaired at 4 °C, but the protein still translocates to the nucleus. **a** Immunoblot of subcellular fractionations of HeLa cells incubated with YopM at 4 °C and 37 °C. In order to assess their purity, fractions were analyzed using antibodies against α-tubulin and LSD1. YopM partition was assessed using a YopM-specific polyclonal antibody. **b** Comparison of the cyto-nuclear YopM ratio at 4 and 37 °C. Immunoblots were densitometrically analyzed using Lumi-Imager T1 and Lumi Analyst software (Roche Diagnostics), normalized by the α-tubulin and LSD1 signals and the cyto-nuclear YopM ratio was calculated. *Error bars* indicate SD. $n = 7$ independent experiments. Student's t test revealed no significant difference between the two means ($p = 0.6$). The cyto-nuclear YopM ratio at 37 and 4 °C is proportional, meaning the reduced amount of nuclear YopM at 4 °C is due to a generally impaired YopM uptake. **c**, **d** Immunoblot of HeLa membrane fractionation after incubation with YopM or Tat-GFP at 4 °C and 37 °C. Membranes were separated using a discontinuous sucrose flotation gradient. The purity of the different fractions was assessed by using marker proteins for different cellular compartments. At 37 °C YopM localized to a high extent in the endosomal fraction. However, even at 4 °C minor amounts of YopM were detectable in the endosome fraction, whereas no Tat-GFP was detectable. **e** Single endosome of the endosomal fraction after a separation in a discontinuous sucrose flotation gradient. The integrity of the endosomes after isolation was confirmed by EM. *Scale bar* 200 nm. *CF* cytosolic fraction, *E* endosomes, *HM* heavy membranes, *LSD1* Lysine-specific demethylase 1, *NF* nuclear fraction, *PNS* post-nuclear supernatant, *PDI* protein disulfide isomerase, *Tat-GFP* fusion protein of the transactivator of transcription and the green fluorescent protein, *TfR* transferrin receptor

is not dependent on endocytosis. As Tat-GFP could not be detected in the endosomal fraction at 4 °C, this feature seems not to be CPP- but YopM-specific.

Discussion

For the detailed investigation of the membrane translocation and intracellular fate of the cell-penetrating, immune-suppressing *Yersinia* effector protein YopM, we employed several distinct and complementary strategies including a morphometric ultra-structural analysis. At physiological temperature, endocytic membranes facilitate the uptake and the intracellular distribution of YopM. Once inside the cell, YopM appears to bypass recycling endosomes and, after targeting EE, is trafficking through the endo-lysosomal pathway to LE. Only a minor part of the detected protein ends up in lysosomes. However, after 1 h of incubation a fraction of YopM is cytosolic and often found in close vicinity to endosomal membranes. Therefore, YopM either has to directly overcome the PM or to escape from endosomes after a targeted vesicular transport towards the nucleus. This process might involve an induced opening of transient pores, back-fusion of intralumenal vesicles from MVB, or an endosomal escape [36]. The results obtained

in our TEM studies using gold-labeled YopM support the hypothesis that the protein traverses the endosomal membranes and, subsequently, the nuclear envelope. In previous studies, recombinant Cy3-labeled YopM appeared to accumulate in the perinuclear region and to colocalize with protein disulfide isomerase (an ER-resident enzyme) [8]. In the present ultra-structural analysis, we could not detect YopM at the ER by TEM, which indicates that the previously observed colocalization by immunofluorescence microscopy might be due to false-positive signals.

However, electron microscopy and biochemical results demonstrated that in addition to endocytic uptake, YopM can enter cells independent of endocytic mechanisms. A block of endocytosis induced by low temperatures resulted in an accumulation of YopM at the outer PM leaflet. This temperature-dependent accumulation has been described also for other cell-penetrating peptides [30]. However, as it is known for Tat, oligoarginine, and other peptides, a non-physiological temperature does not preclude YopM from penetrating the cellular barrier [37]. The total amount of intracellular YopM at 4 °C was somewhat lower compared to the amount that was observed at physiological temperatures. However, inhibition of the endosomal pathway still resulted in a considerable translocation of YopM to the cytosol. This indicates that YopM can penetrate eukaryotic cells by at least two different probably parallel mechanisms: endocytosis and direct penetration of the PM. As a non-penetrative deletion construct ($YopM_{87\text{-}C}$) lacking the N-terminal protein transduction domain of YopM (7) is still endocytosed at 37 °C but not at 4 °C (Fig. S1), it is most likely that the acidic and "sticky" LRRs of the protein mediate a non-specific interaction with the negatively charged surface of the PM, which in turn facilitates endocytosis of the effector protein. As the inner leaflet of endosomal membranes corresponds to the outer leaflet of the PM, YopM's ability to directly traverse the PM suggests that after endocytosis the protein might be able to escape the endosomal compartment by a similar mechanism.

In order to investigate if YopM enters cells independently of a host-cell receptor, cell surface proteins were removed by proteinase K treatment prior to YopM (25 µg/ml) incubation and analysis by flow cytometry. These FACS analyses revealed that YopM still enters HeLa cells after they have been treated with PK, while uptake of transferrin was almost completely abolished under the same conditions (Fig. S3a, b). These experiments were underlined by additional subcellular fractionations of HeLa cells incubated with YopM after removal of cell surface proteins by PK (Fig. S3c). Taken together, these data show that cellular surface receptors are most likely not essential for penetration of host cells by YopM. However, a slight decrease of YopM uptake after PK treatment might indicate that some surface proteins could facilitate the initial contact of the effector protein with the plasma membrane, which in turn might lead to higher penetration rates.

With respect to the ongoing controversial discussion about the various different internalization modes proposed for CPPs, there seems to be a general consensus now that the same CPPs are able to use different mechanisms simultaneously to penetrate cellular membranes [16, 38]. How these mechanisms depend on the structure of the CPP and its particular environment remains unresolved [33]. However, the advantage of endocytosis prior to the endosomal escape of YopM might result in an enlargement of penetrable membrane surface for the effector protein and in turn in a higher internalization rate.

Strikingly, at 37 °C as well as at 4 °C cytosolic YopM was often found to be associated with endosomal membranes with a preference for LE. This apparent tropism of YopM, which predominantly involves the attachment to the vesicle or endosomal surface but also the observed intra-endosomal localization at 4 °C, might enable the protein to utilize the endosomal movement for its intracellular trafficking. This mechanism is presumably not only associated with isolated recombinant YopM but most likely also occurs during a *Yersinia* infection. This is supported by the finding first described by Skrzypek et al. that after a T3SS-mediated translocation of Yops into the host cell cytosol, YopM reaches the nucleus by means of a vesicle-associated pathway [4]. This was further confirmed for the trafficking of YopM from *Y. pestis* in the yeast *Saccharomyces cerevisiae* [39]. As we could not detect any Tat peptide in the endosomal fraction after incubation of HeLa cells at 4 °C, we conclude that this transport mechanism is not characteristic for CPPs but rather specific for YopM.

In accordance with the subcellular localization of YopM during a *Yersinia* infection [4, 5], we could show that recombinant YopM, after overcoming the PM, translocates into the HeLa cell nucleus as had been shown previously after transfection and subsequent expression of YopM from *Y. pestis* in *S. cerevisiae* [39]. This demonstrates that no other bacterial factors are required for the translocation of the protein into the nucleus. In addition to this, we could further demonstrate that not even transfection is necessary for the intracellular trafficking of recombinant YopM to the nucleus. Solely adding the recombinant protein to the culture medium results in the autonomous penetration of the PM and subsequent trafficking of YopM to the cell nucleus. Thus far, YopM is the only *Yersinia* effector protein that translocates to the nucleus. Two putative NLS have been identified within the *Y. enterocolitica* YopM sequence, encompassing $LRRs_{1\text{-}3}$ and 32 amino acid residues of the C-terminus, which do not correspond to a known NLS [5]. However, the mechanism of YopM's translocation into the

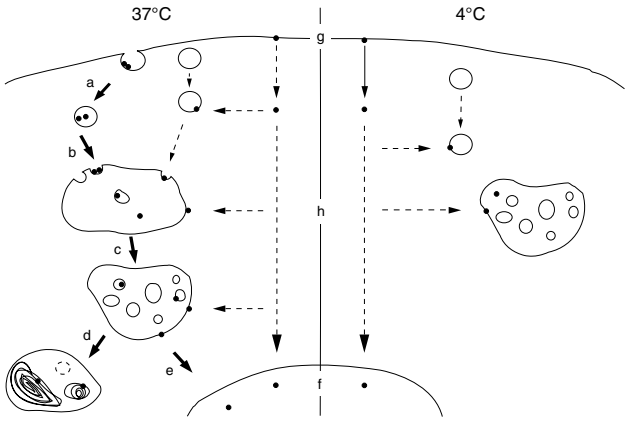

Fig. 8 Model of YopM′s transduction and possible transport pathways. **a** At physiological temperature, the endocytic membranes facilitate the uptake and distribution of YopM. The protein is transported through early (**b**) and late (**c**) endosomes and fractionally to lysosomes (**d**). Entrapped YopM seems to be able to escape from endocytotic membranes (**e**) and to reach the nucleus (**f**). At 4 °C YopM directly penetrates the PM (**g**), which might also be a possible mechanism at 37 °C. Cytosolic YopM shows a tropism towards endosomal compartments (**h**) and the attachment to the vesicle surface might enable the protein to achieve its intracellular distribution. *Dashed arrows* indicate possible intracellular YopM movement. *Filled arrows* show confirmed YopM transduction and transport

nucleus has not been elucidated yet, although a carrier-mediated translocation mechanism has been suggested by Skrzypek et al. [4].

The results of this study are summarized in a model depicting the possible entry mechanisms of the CPP YopM (Fig. 8). At physiological temperatures, YopM is predominantly endocytosed and reaches the cytosol by escaping from endosomes. Furthermore, at 37 °C, a fraction of YopM appears to directly penetrate the cellular PM. Strikingly, when endocytosis is blocked at 4 °C, YopM is entering the cell by directly penetrating the cellular lipid bilayer. However, at 4 °C, the total amount of recombinant protein entering the cell is lower, which in turn leads to a reduced nuclear accumulation of YopM compared to the translocation at 37 °C. Independent of the incubation temperature, YopM interacts with vesicular as well as endosomal membranes, which might serve the protein to traffic towards the nucleus.

In summary, our results document critical uptake and targeting mechanisms of the novel bacterial CPP YopM, which form the basis for an efficient down-regulation of the expression of several pro-inflammatory cytokines including TNF-α [8]. Furthermore, the elucidation of intracellular trafficking pathways of YopM from *Y. enterocolitica* strain 8081 (serotype 0:8; biotype 1B) in this study will contribute to and facilitate its further development as a potential biologic anti-inflammatory therapeutic. However, in future studies it has to be investigated whether also YopM molecules from other species or serotypes, e.g., *Y. pestis* or *Y. pseudotuberculosis*, which vary in the number of their LRRs, follow the same intracellular trafficking pathways as the protein used in this study.

Acknowledgments This study was supported in part by the Graduate Program "Cell Dynamics and Disease (CEDAD)" of the Westfälische Wilhelms-Universität Münster (9817300 to J. S.) and by the Deutsche Forschungsgemeinschaft (Graduiertenkolleg GRK 1409) (209657 to M. A. S. and M.-L. L.) and by a grant of the Innovative Medizinische Forschung (IMF) (I-RÜ11106 to C. R.). This study is part of the PhD thesis of J. S. and M.-L. L.

References

1. Forsberg A, Viitanen AM, Skurnik M, Wolf-Watz H (1991) The surface-located YopN protein is involved in calcium signal transduction in *Yersinia pseudotuberculosis*. Mol Microbiol 5:977–986
2. Straley SC, Bowmer WS (1986) Virulence genes regulated at the transcriptional level by Ca2 + in *Yersinia pestis* include structural genes for outer membrane proteins. Infect Immun 51:445–454
3. Boland A, Havaux S, Cornelis GR (1998) Heterogeneity of the *Yersinia* YopM protein. Microb Pathog 25:343–348
4. Skrzypek E, Cowan C, Straley SC (1998) Targeting of the *Yersinia* pestis YopM protein into HeLa cells and intracellular trafficking to the nucleus. Mol Microbiol 30:1051–1065
5. Benabdillah R, Mota LJ, Lützelschwab S, Demoinet E, Cornelis GR (2004) Identification of a nuclear targeting signal in YopM from *Yersinia* spp. Microb Pathog 36:247–261
6. Kerschen EJ, Cohen DA, Kaplan AM, Straley SC (2004) The plague virulence protein YopM targets the innate immune response by causing a global depletion of NK cells. Infect Immun 72:4589–4602
7. Ye Z, Uittenbogaard AM, Cohen DA, Kaplan AM, Ambati J et al (2011) Distinct CCR2(+) Gr1(+) cells control growth of the *Yersinia* pestis ΔyopM mutant in liver and spleen during systemic plague. Infect Immun 79:674–687
8. Rüter C, Buss C, Scharnert J, Heusipp G, Schmidt MA (2010) A newly identified bacterial cell-penetrating peptide that reduces the transcription of pro-inflammatory cytokines. J Cell Sci 123:2190–2198
9. Kilk K, Langel U (2005) Cellular delivery of peptide nucleic acid by cell-penetrating peptides. Methods Mol Biol 298:131–141
10. Holm T, Andaloussi SE, Langel U (2011) Comparison of CPP uptake methods. Methods Mol Biol 683:207–217
11. Richard JP, Melikov K, Brooks H, Prevot P, Lebleu B et al (2005) Cellular uptake of unconjugated TAT peptide involves clathrin-dependent endocytosis and heparan sulfate receptors. J Biol Chem 280:15300–15306
12. Fischer R, Fotin-Mleczek M, Hufnagel H, Brock R (2005) Break on through to the other side-biophysics and cell biology shed light on cell-penetrating peptides. Chem BioChem 6: 2126–2142
13. Kaplan IM, Wadia JS, Dowdy SF (2005) Cationic TAT peptide transduction domain enters cells by macropinocytosis. J Control Release 102:247–253
14. Wadia JS, Stan RV, Dowdy SF (2004) Transducible TAT-HA fusogenic peptide enhances escape of TAT-fusion proteins after lipid raft macropinocytosis. Nat Med 10:310–315
15. Säälik P, Padari K, Niinep A, Lorents A, Hansen M et al (2009) Protein delivery with transportans is mediated by caveolae rather than flotillin-dependent pathways. Bioconjug Chem 20: 877–887

16. Duchardt F, Fotin-Mleczek M, Schwarz H, Fischer R, Brock R (2007) A comprehensive model for the cellular uptake of cationic cell-penetrating peptides. Traffic 8:848–866
17. Tünnemann G, Martin RM, Haupt S, Patsch C, Edenhofer F et al (2006) Cargo-dependent mode of uptake and bioavailability of TAT-containing proteins and peptides in living cells. FASEB J 20:1775–1784
18. Heusipp G, Spekker K, Brast S, Fälker S, Schmidt MA (2006) YopM of *Yersinia enterocolitica* specifically interacts with alpha1-antitrypsin without affecting the anti-protease activity. Microbiology 152:1327–1335
19. el Bayâ A, Linnermann R, von Olleschik-Elbheim L, Schmidt MA (1997) Pertussis toxin. Entry into cells and enzymatic activity. Adv Exp Med Biol 419:83–86
20. Mari M, Bujny MV, Zeuschner D, Geerts WJ, Griffith J et al (2008) SNX1 defines an early endosomal recycling exit for sortilin and mannose 6-phosphate receptors. Traffic 9:380–393
21. Langel Ü (2005) Handbook of cell-penetrating peptides. CRC Press, Taylor & Francis Group, Boca Raton
22. Gorvel JP, Chavrier P, Zerial M, Gruenberg J (1991) rab5 controls early endosome fusion in vitro. Cell 64:915–925
23. Brown E, Verkade P (2010) The use of markers for correlative light electron microscopy. Protoplasma 244:91–97
24. Hutagalung AH, Novick PJ (2011) Role of Rab GTPases in membrane traffic and cell physiology. Physiol Rev 91:119–149
25. Rink J, Ghigo E, Kalaidzidis Y, Zerial M (2005) Rab conversion as a mechanism of progression from early to late endosomes. Cell 122:735–749
26. Lombardi D, Soldati T, Riederer MA, Goda Y, Zerial M et al (1993) Rab9 functions in transport between late endosomes and the trans Golgi network. EMBO J 12:677–682
27. Goud B, Zahraoui A, Tavitian A, Saraste J (1990) Small GTP-binding protein associated with Golgi cisternae. Nature 345:553–556
28. Trabulo S, Resina S, Simões S, Lebleu B, Pedroso de Lima MC (2010) A non-covalent strategy combining cationic lipids and CPPs to enhance the delivery of splice correcting oligonucleotides. J Control Release 145:149–158
29. Ter-Avetisyan G, Tünnemann G, Nowak D, Nitschke M, Herrmann A et al (2009) Cell entry of arginine-rich peptides is independent of endocytosis. J Biol Chem 284:3370–3378
30. Jiao CY, Delaroche D, Burlina F, Alves ID, Chassaing G et al (2009) Translocation and endocytosis for cell-penetrating peptide internalization. J Biol Chem 284:33957–33965
31. Weigel PH, Oka JA (1981) Temperature dependence of endocytosis mediated by the asialoglycoprotein receptor in isolated rat hepatocytes. Evidence for two potentially rate-limiting steps. J Biol Chem 256:2615–2617
32. Letoha T, Gaál S, Somlai C, Czajlik A, Perczel A et al (2003) Membrane translocation of penetratin and its derivatives in different cell lines. J Mol Recognit 16:272–279
33. Padari K, Säälik P, Hansen M, Koppel K, Raid R et al (2005) Cell transduction pathways of transportans. Bioconjug Chem 16:1399–1410
34. Frankel AD, Pabo CO (1988) Cellular uptake of the tat protein from human immunodeficiency virus. Cell 55:1189–1193
35. Green M, Loewenstein PM (1988) Autonomous functional domains of chemically synthesized human immunodeficiency virus tat trans-activator protein. Cell 55:1179–1188
36. Medina-Kauwe LK (2007) Alternative endocytic mechanisms exploited by pathogens: new avenues for therapeutic delivery? Adv Drug Deliv Rev 59:798–809
37. Derossi D, Calvet S, Trembleau A, Brunissen A, Chassaing G et al (1996) Cell internalization of the third helix of the Antennapedia homeodomain is receptor-independent. J Biol Chem 271:18188–18193
38. Heitz F, Morris MC, Divita G (2009) Twenty years of cell-penetrating peptides: from molecular mechanisms to therapeutics. Br J Pharmacol 157:195–206
39. Lesser CF, Miller SI (2001) Expression of microbial virulence proteins in *Saccharomyces cerevisiae* models mammalian infection. EMBO J 20:1840–1849